ChemComm

COMMUNICATION

View Article Online
View Journal | View Issue

Cite this: *Chem. Commun.*, 2019, 55, 401

Received 7th November 2018,
Accepted 4th December 2018

DOI: 10.1039/c8cc08868c

rsc.li/chemcomm

Synthesis and nitric oxide releasing properties of novel fluoro *S*-nitrosothiols†

Yang Zhou,[a] Jinyi Tan,[a] Yuping Dai,[b] Yanmin Yu,[b] Qi Zhang[a] and Mark E. Meyerhoff*[a]

A series of new fluoro *S*-nitrosothiols is reported as potential nitric oxide (NO) donors. A three-step synthesis and the NO releasing kinetic profiles of these species are presented. The stoichiometric release of NO, with the clean formation of corresponding disulfides, confirms that these new species can facilitate their application as NO donors for various applications including creating novel antimicrobial and thromboresistant fluoropolymer-based medical devices.

Nitric oxide (NO), an endogenous signaling molecule,[1–3] has been extensively studied for its vasodilatory,[4] antithrombotic,[5] immune modulatory,[6] antimicriobial,[7] anticancer[8] and wound healing[9] properties. However, due to its high reactivity, the intravascular lifetime of NO is very short (~2 s).[10] Therefore, precursor molecules (NO donors) are commonly utilized to generate NO *in situ* for chemical and biochemical studies. So far, various NO donors have been reported,[11] including *S*-nitrosothiols, *N*-diazeniumdiolates and their derivatives, metal nitrosyls, and *N*-nitrosamines, as well as organic nitrates and nitrites. Current NO donors are also widely investigated as promising medicinal and therapeutic agents for disease treatments.[12–14]

Fluorine-containing compounds have significant potential applications in medical and materials chemistry.[15,16] In pharmaceuticals, almost 150 fluorinated drugs have successfully reached the market since the first fluorine-containing drug (fludrocortisone) was approved in 1955.[16] Currently, 20–30% administered drugs contain fluorine atoms or fluoroalkyl groups.[16] Fluorocarbon-based materials also have been widely applied in clinical biomaterials,[17] affinity chromatography,[18] enzyme immobilization,[19] crystal engineering[20] and supermolecular chemistry.[21] Overall, the development of fluorinated compounds and materials with desired functionalities is of continuous interest and has significance in all branches of chemistry.

In the recent development of NO-releasing polymers for use in preparing implanted antimicrobial and thromboresistant biomedical devices (*e.g.*, intravascular catheters, subcutaneous cannula, *etc.*), chemical leaching of the NO donor and its decomposition products has become a critical concern, owing to possible toxicity issues.[22] Very recently, our group reported the incorporation of a novel fluorinated NO donor (*S*-nitroso-*N*-pentafluoropropionyl-penicillamine, C_2F_5-SNAP) into polyvinylidene fluoride for preparation of fluoropolymer-based biomaterials that exhibit NO release and significant antimicrobial properties.[23] Due to the specific fluorous–fluorous interactions present between the fluorinated NO donor and the fluoropolymer, leaching of the fluorinated NO donor and the corresponding decomposition products was demonstrated to be quite low (<10%, total), compared to that observed in the use of non-fluorinated NO donors. Thus, the development of new fluorinated NO donors is of great interest for potentially creating fluoropolymer-based NO release biomaterials from which chemical leaching will be greatly reduced for potential applications of biomedical implants and devices.

To the best of our knowledge, fluorinated *S*-nitrosothiol type NO donors have not received much attention in the medical and biomaterials research fields. Indeed, to date, only the C_2F_5-SNAP molecule has been reported as a fluorinated NO donor.[23] However, the C_2F_5-SNAP NO donor was found to be quite unstable even upon storage within a freezer, resulting in the difficulty in handling and storage of this species.[23] In contrast, the non-fluorinated *S*-nitroso-*N*-acetylpenicillamine (SNAP, see Fig. 1) has great stability, and has extensively been doped into various polymers for the long-term NO release over several months.[22] Therefore, there is a need to develop new and relatively stable fluorinated structural analogs of SNAP as NO donors for fluoropolymer-based biomedical devices applications.

Herein, we consider the amine-based nucleophilic addition chemistry of thiolactone (see Fig. 1), which has been widely used to incorporate free thiol moieties as the precursors of *S*-nitrosothiols.[24–27] 3-Acetamido-4,4-dimethylthietan-2-one

[a] *Department of Chemistry, University of Michigan, Ann Arbor, MI 48109, USA. E-mail: mmeyerho@umich.edu*
[b] *Beijing Key Laboratory for Green Catalysis and Separation, Department of Chemistry and Chemical Engineering, Beijing University of Technology, Beijing 100124, China*

† Electronic supplementary information (ESI) available: Experimental details. See DOI: 10.1039/c8cc08868c

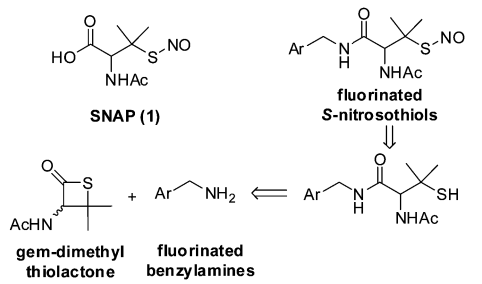

Fig. 1 Chemical structure of SNAP and the design of fluorinated *S*-nitrosothiols from thiolactone.

(*gem*-dimethyl thiolactone) was selected as the thiolactone to imitate the structure of SNAP. To prevent the strong electron withdrawing effects from fluorine or fluoroalkyl groups on the stability of S–N bond, we consider fluorinated benzylamine derivatives as nucleophiles. Specifically, the phenyl ring acts as a linker to diminish the strong electron withdrawing effects from fluoro/trifluoromethyl groups. We hypothesize that a nucleophilic ring opening of the thiolactone in the presence of fluorinated benzylamines should yield amide-based tertiary free thiols, which can be subsequently nitrosylated into fluorinated *S*-nitrosothiols (see Fig. 1).

In total, 12 fluorinated benzylamines with various degrees of fluorine substitution and 2 non-fluorinated benzylamines were utilized in the synthesis of the new amide-based *S*-nitrosothiols shown in Scheme 1. The *gem*-dimethyl thiolactone intermediate was easily obtained from the reaction between D-penicillamine and excess acetic anhydride. In the presence of various benzylamines as nucleophiles, a ring opening of the *gem*-dimethyl thiolactone yielded amide-based free thiol **2** intermediates. With pure thiol intermediates **2** in hand, a nitrosylation reaction using $NaNO_2$ in presence of strong acid under dark conditions yielded the pure target products **3a–3n** as greenish powders. NO donors **3a–3n** were obtained with total yields of between 21–30% in three steps (see Section S2 in ESI†).

Although *S*-nitrosothiols are known to be relatively unstable due to the inherently weak S–N bond (25–31 kcal mol^{-1}),[28,29] SNAP is very stable at room temperature. For the previously prepared C_2F_5-SNAP NO donor, due to the presence of fluorinated groups, C_2F_5-SNAP was found to be unstable at room temperature and even slowly decompose at −20 °C.[23] All new targets **3a–3n** were found to be stable during the vacuum drying process at room temperature in the dark. Additionally, they remained stable after being stored at −20 °C over several months. For example, ^{1}H NMR studies of **3l** indicated that no decomposition of **3l** was observed after storage for 40 days at −20 °C under dark conditions (see Fig. S1, ESI†). Hence, the presence of fluoro/trifluoromethyl groups on the aromatic ring in targets **3a–3n** do not appear to decrease the stability of the resulting *S*-nitrosothiols as observed for C_2F_5-SNAP. This result is also consistent with the literature finding that tertiary *S*-nitrosothiols are known to be thermally stable.[29]

To further investigate the NO release profiles from **3a–3n**, we carried out kinetic studies of their photolytic and thermal decompositions. For example, the steady-state photolysis of **3k** (150 μM) was carried out under 350 nm irradiation in a mixture of PBS and DMSO (50 : 50, v/v) at 23 °C. The UV-Vis spectra of its photo-decomposition are shown in Fig. 2a, in which the characteristic UV-Vis band of the $n_O \rightarrow \pi^*$ transition (342 nm) continuously decreases and eventually flattens. The kinetic profile was analyzed using the absorbance changes at 342 nm (Fig. 2a inset), and was fitted to a first-order rate equation giving an observed rate constant $k_{obs} = (1.214 \pm 0.052) \times 10^{-2}$ s^{-1} ($t_{1/2} \sim 57$ s). The corresponding rate constants and half-lives for the photo-decomposition of the other NO donors synthesized in this work are summarized in Table 1. All exhibit first-order decomposition with half-lives between 50 to 80 s under light irradiation. Compared to the photostability of SNAP ($t_{1/2} \sim 46$ s), **3a–3n** exhibit slower photo-decomposition rates. Targets **3m** and **3n** have similar decomposition rate constants to **3a–3l**, indicating that substitution groups on the phenyl ring do not influence the photolytic release rate of NO.

Thermal decomposition studies of **3a–3n** at 37 °C were also performed in a mixture of PBS and DMSO (50 : 50, v/v). The absorbance data *vs.* time for the decomposition of **3k** at 342 nm (see Fig. 2b) was monitored and this kinetic data was fitted to a zero-order rate equation, yielding an observed rate constant k_{obs} of $(1.446 \pm 0.001) \times 10^{-4}$ μM min^{-1}. All of the thermal decomposition kinetic data for compounds **1** and **3a–3n** are reported in Table 2. NO donors **3a–3n** are less stable in solution when compared to SNAP. NO donors **3d–3e** and **3j–3l** decomposed *via* a zero-order reaction model, similar to SNAP. But the others, **3a–3c**, **3f–3i** and **3m–3n**, exhibit first-order decomposition kinetics.

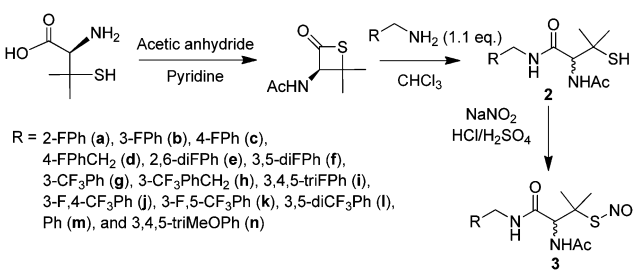

Scheme 1 Synthesis of NO donors **3a–3n**.

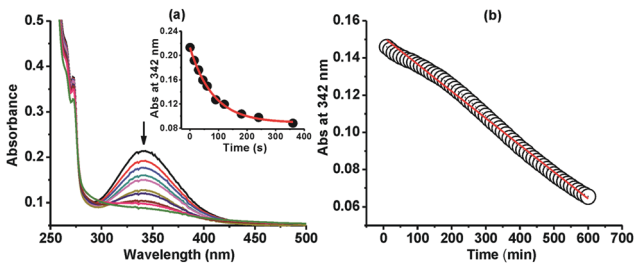

Fig. 2 (a) UV/Vis spectra for the photolysis of **3k** (150 μM) at 23 °C in a mixture of PBS and DMSO (50 : 50, v/v). Inset: Plot of absorbance at 342 nm *vs.* time and fitting into a first-order rate equation. (b) Plot of absorbance at 342 nm *vs.* time for the thermal decomposition of **3k** (100 μM) at 37 °C in a mixture of PBS and DMSO (50 : 50, v/v).

Table 1 Kinetic photo-decomposition data for NO donors **1** and **3a–3n** under irradiation of 350 nm (4 W) in a mixture of PBS and DMSO (50 : 50, v/v) at 23 °C

NO donors	Rate constant (s^{-1})	Half-lives (s)
1 (250 μM)	$(1.495 \pm 0.027) \times 10^{-2}$	46
3a (250 μM)	$(0.945 \pm 0.031) \times 10^{-2}$	73
3b (250 μM)	$(1.006 \pm 0.023) \times 10^{-2}$	69
3c (250 μM)	$(1.012 \pm 0.063) \times 10^{-2}$	68
3d (250 μM)	$(1.384 \pm 0.046) \times 10^{-2}$	50
3e (250 μM)	$(1.047 \pm 0.050) \times 10^{-2}$	66
3f (250 μM)	$(0.911 \pm 0.022) \times 10^{-2}$	76
3g (250 μM)	$(1.009 \pm 0.013) \times 10^{-2}$	69
3h (250 μM)	$(0.864 \pm 0.017) \times 10^{-2}$	80
3i (250 μM)	$(1.011 \pm 0.015) \times 10^{-2}$	69
3j (150 μM)	$(1.191 \pm 0.071) \times 10^{-2}$	58
3k (150 μM)	$(1.214 \pm 0.052) \times 10^{-2}$	57
3l (250 μM)	$(1.177 \pm 0.075) \times 10^{-2}$	58
3m (250 μM)	$(0.972 \pm 0.030) \times 10^{-2}$	71
3n (250 μM)	$(1.020 \pm 0.034) \times 10^{-2}$	68

Table 2 Thermal decomposition kinetic data of NO donors **1** and **3a–3n** at 37 °C in a mixture of PBS and DMSO (50 : 50, v/v)

NO donors	Rate constant	Half-lives (h)
1 (100 μM)	$(1.586 \pm 0.012) \times 10^{-5}$ μM min^{-1}	56.22
3a (250 μM)	$(2.070 \pm 0.027) \times 10^{-3}$ min^{-1}	5.58
3b (250 μM)	$(2.720 \pm 0.021) \times 10^{-3}$ min^{-1}	4.25
3c (250 μM)	$(2.480 \pm 0.036) \times 10^{-3}$ min^{-1}	4.66
3d (100 μM)	$(8.395 \pm 0.028) \times 10^{-5}$ μM min^{-1}	6.45
3e (100 μM)	$(4.685 \pm 0.001) \times 10^{-5}$ μM min^{-1}	15.47
3f (250 μM)	$(2.290 \pm 0.104) \times 10^{-3}$ min^{-1}	5.04
3g (250 μM)	$(2.180 \pm 0.082) \times 10^{-3}$ min^{-1}	5.30
3h (150 μM)	$(1.970 \pm 0.039) \times 10^{-3}$ min^{-1}	5.86
3i (250 μM)	$(2.130 \pm 0.114) \times 10^{-3}$ min^{-1}	5.42
3j (100 μM)	$(1.366 \pm 0.011) \times 10^{-4}$ μM min^{-1}	4.70
3k (100 μM)	$(1.446 \pm 0.001) \times 10^{-4}$ μM min^{-1}	5.24
3l (100 μM)	$(8.089 \pm 0.062) \times 10^{-5}$ μM min^{-1}	6.49
3m (250 μM)	$(2.010 \pm 0.090) \times 10^{-3}$ min^{-1}	5.75
3n (250 μM)	$(2.520 \pm 0.075) \times 10^{-3}$ min^{-1}	4.58

To understand these different kinetic behaviors, we also performed computational calculations (see Section S5 in ESI†). Interestingly, the transition state for the homolysis of the S–N bond resulting in NO release does not exist. We found experimentally that the NO release was mainly determined by the calculated binding dissociation enthalpy (BDE) of S–N bond. Compared to SNAP, **3e**, **3l** and **3m** have slightly lower BDE (see Table S3, ESI†) for the S–N bond. Thus, **3e**, **3l** and **3m** are less stable than SNAP, consistent with our kinetic results under the thermal decomposition.

Furthermore, the emitted NO gas released by each new donor was accurately quantitated by an NOA chemiluminescence method. For instance, the photolysis of **3k** (1.50×10^{-7} mol) within a NOA reaction cell was conducted in a mixture of PBS and DMSO (50 : 50, v/v) under 350 nm lamp irradiation, in which the corresponding NO gas signal was monitored by the NOA analyzer (see Fig. 3a). Three independent photolysis reactions gave the average NO generation yield of 98 ± 2%. These results indicate that NO donor **3k** can stoichiometrically release NO.

In addition to NO gas, the corresponding disulfide is reported to be the product derived from the decomposition of

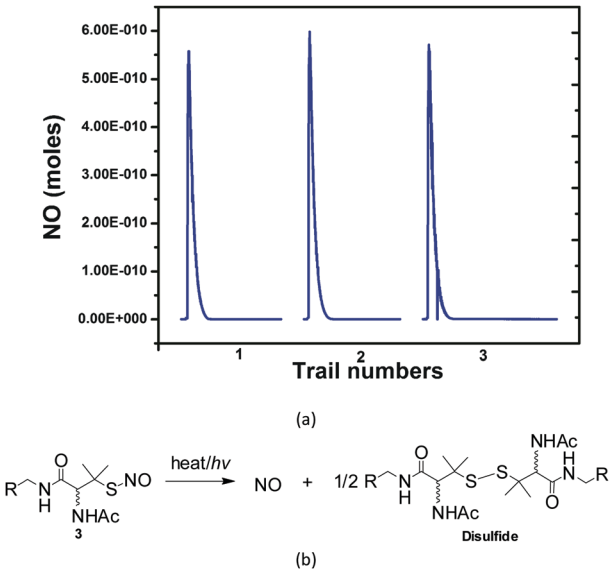

Fig. 3 (a) Stoichiometric NO determination observed for photolysis of **3k** (1.50×10^{-7} mol) using chemiluminescence NOA detection of emitted NO in a mixture of PBS (10.0 mM, pH 7.40, with 100 μM EDTA) and DMSO (50 : 50, v/v) at 23 °C, and (b) NO release reaction for NO donors **3**.

S-nitrosothiols.[30] To further examine the disulfide formation, products derived from both the photo and thermal decomposition of **3k** (2.98 mM) in DMSO-d_6 were analyzed by ^{1}H NMR spectroscopy (see Fig. 4). Before the decomposition, methide and *gem*-dimethyl groups in **3k** had chemical shifts at ~5.30, 1.98 and 1.96 ppm. After photolysis for 2 h, **3k** was completely decomposed, to cleanly yield the disulfide, with the methide resonance at ~4.65 ppm and *gem*-dimethyl groups at ~1.33 and 1.25 ppm. This disulfide was further confirmed by HRMS results (*m*/*z* (ESI): calculated for $[M + H]^+$ = 731.1966; found = 731.1965). Interestingly, a partial thermal decomposition of **3k** was observed after 4 d at 37 °C in the dark (see Fig. 4), yielding a mixture of **3k** and its corresponding disulfide. These data provide evidence that **3k** can be employed as a pure NO donor, to stoichiometrically release NO and the corresponding disulfide. The mechanism of NO-release from *S*-nitrosothiols has been

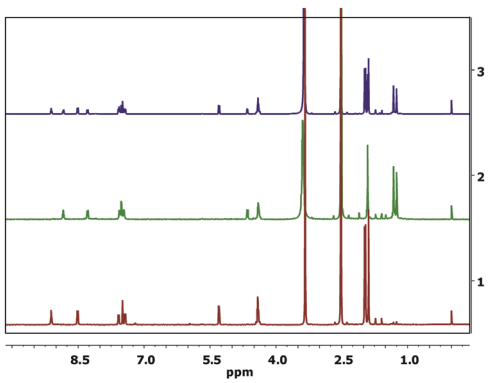

Fig. 4 ^{1}H NMR spectra for **3k** (2.98 mM) before and after decomposition in DMSO-d_6 (1) before decomposition, (2) after photolysis at 23 °C for 2 h, (3) after thermal decomposition at 37 °C in the dark for 4 d.

well-studied under heat, irradiation, and Cu^{+} mediated reduction conditions.[28,30] A homolysis of the weak S–N bond could yield equal moles of NO and a thiyl radical. Thiyl radical intermediates are typically reactive, subsequently resulting in a rapid dimerization to yield the corresponding disulfide.[28,30] Finally, a possible NO generation pathway for NO donors **3** is summarized in Fig. 3b, based on our NO measurement and disulfide characterization.

To summarize, a novel family of fluorinated *S*-nitrosothiols has been reported herein. The presence of fluorine or fluoroalkyl groups on the benzylamide does not influence the stability of the S–N bond. Kinetic studies of their photolytic and thermal decomposition reactions were conducted. The stoichiometric release of NO and the corresponding disulfide formation from decomposition was monitored by NO chemiluminescence measurements and ^{1}H NMR spectroscopy, respectively. Detailed theoretical calculations on the relationship between structure and stability of these new fluorinated NO donors are currently underway. We anticipate that these new species will have applications as useful NO release agents, potentially for incorporation into fluorinated biopolymers for preventing infection and/or thrombosis on surfaces of various medical devices. Such studies are now ongoing in our laboratory.

The authors acknowledge the Juvenile Diabetes Research Foundation (JDRF: 2-SRA-2016-230-Q-R) and the National Institutes of Health (HL-128337) for supporting this research. We also are grateful to Dr. Paul Sampson at Kent State University for helpful discussion on fluorine chemistry.

Conflicts of interest

There are no financial conflicts to declare.

Notes and references

1 T. A. Heinrich, R. S. da Silva, K. M. Miranda, C. H. Switzer, D. A. Wink and J. M. Fukuto, *Br. J. Pharmacol.*, 2013, **169**, 1417–1429.
2 D. D. Thomas, *Redox Biol.*, 2015, **5**, 225–233.
3 C. Farah, L. Y. M. Michel and J.-L. Balligand, *Nat. Rev. Cardiol.*, 2018, **15**, 292.
4 M. J. Simmonds, J. A. Detterich and P. Connes, *Biorheology*, 2014, **51**, 121–134.
5 T. Constantine and E. F. Jane, *Curr. Drug Targets*, 2006, **7**, 1243–1251.
6 C. Bogdan, *Trends Immunol.*, 2015, **36**, 161–178.
7 L. Yang, E. S. Feura, M. J. R. Ahonen and M. H. Schoenfisch, *Adv. Healthcare Mater.*, 2018, **7**, 1800155.
8 V. Huzefa, K. Munawwar Ali, A. Usama and H. Arif, *J. Cancer Prev.*, 2016, **21**, 1–12.
9 A. Krausz and A. J. Friedman, *Future Sci. OA*, 2015, **1**, FSO56.
10 X. Liu, M. J. S. Miller, M. S. Joshi, H. Sadowska-Krowicka, D. A. Clark and J. R. Lancaster, *J. Biol. Chem.*, 1998, **273**, 18709–18713.
11 P. G. Wang, M. Xian, X. Tang, X. Wu, Z. Wen, T. Cai and A. J. Janczuk, *Chem. Rev.*, 2002, **102**, 1091–1134.
12 A. D. Ostrowski and P. C. Ford, *Dalton Trans.*, 2009, 10660–10669.
13 Z. Huang, J. Fu and Y. Zhang, *J. Med. Chem.*, 2017, **60**, 7617–7635.
14 T. Munzel and A. Daiber, *Vasc. Pharmacol.*, 2018, **102**, 1–10.
15 R. Berger, G. Resnati, P. Metrangolo, E. Weber and J. Hulliger, *Chem. Soc. Rev.*, 2011, **40**, 3496–3508.
16 Y. Zhou, J. Wang, Z. Gu, S. Wang, W. Zhu, J. L. Aceña, V. A. Soloshonok, K. Izawa and H. Liu, *Chem. Rev.*, 2016, **116**, 422–518.
17 V. Cardoso, D. Correia, C. Ribeiro, M. Fernandes and S. Lanceros-Méndez, *Polymers*, 2018, **10**, 161.
18 T. Hayama, H. Yoshida, M. Yamaguchi and H. Nohta, *J. Pharm. Biomed. Anal.*, 2014, **101**, 151–160.
19 H. M. Rapp, S. Bacher, A. Ahrens, W. Rapp, B. Kammerer, G. U. Nienhaus and W. Bannwarth, *ChemPlusChem*, 2012, **77**, 1066–1070.
20 D. Chopra and T. N. G. Row, *CrystEngComm*, 2011, **13**, 2175–2186.
21 H. Omorodion, B. Twamley, J. A. Platts and R. J. Baker, *Cryst. Growth Des.*, 2015, **15**, 2835–2841.
22 Y. Wo, E. J. Brisbois, R. H. Bartlett and M. E. Meyerhoff, *Biomater. Sci.*, 2016, **4**, 1161–1183.
23 Y. Zhou, Q. Zhang, J. Wu, C. Xi and M. E. Meyerhoff, *J. Mater. Chem. B*, 2018, **6**, 6142–6152.
24 L. Soulère, J.-C. Sturm, L. J. Núñez-Vergara, P. Hoffmann and J. Périé, *Tetrahedron*, 2001, **57**, 7173–7180.
25 M. C. Frost and M. E. Meyerhoff, *J. Am. Chem. Soc.*, 2004, **126**, 1348–1349.
26 N. A. Stasko, T. H. Fischer and M. H. Schoenfisch, *Biomacromolecules*, 2008, **9**, 834–841.
27 B. M. Grommersch, J. Pant, S. P. Hopkins, M. J. Goudie and H. Handa, *ACS Appl. Mater. Interfaces*, 2018, **10**, 2291–2301.
28 D. L. H. Williams, *Chem. Commun.*, 1996, 1085–1091.
29 D. L. H. Williams, *Acc. Chem. Res.*, 1999, **32**, 869–876.
30 C. Zhang, T. D. Biggs, N. O. Devarie-Baez, S. Shuang, C. Dong and M. Xian, *Chem. Commun.*, 2017, **53**, 11266–11277.

